

# A geometric reappraisal of proximal landing zones for thoracic endovascular aortic repair according to aortic arch types

Massimiliano M. Marrocco-Trischitta, MD, PhD,<sup>a,b</sup> Hector W. de Beaufort, MD,<sup>b</sup> Francesco Secchi, MD,<sup>c</sup> Theodorus M. van Bakel, MD,<sup>b</sup> Marco Ranucci, MD,<sup>d</sup> Joost A. van Herwaarden, MD, PhD,<sup>e</sup> Frans L. Moll, MD, PhD,<sup>e</sup> and Santi Trimarchi, MD, PhD,<sup>a,b</sup> *San Donato Milanese, Italy; and Utrecht, The Netherlands*

## ABSTRACT

**Objective:** This study assessed whether the additional use of the aortic arch classification in type I, II, and III may complement Ishimaru's aortic arch map and provide valuable information on the geometry and suitability of proximal landing zones for thoracic endovascular aortic repair.

**Methods:** Anonymized thoracic computed tomography scans of healthy aortas were reviewed and stratified according to the aortic arch classification, and 20 of each type of arch were selected. Further processing allowed calculation of angulation and tortuosity of each proximal landing zone. Data were described indicating both proximal landing zone and type of arch (eg, 0/I).

**Results:** Angulation was severe ( $>60^\circ$ ) in 2/III and in 3/III. Comparisons among the types of arch showed an increase in proximal landing zones angulation ( $P < .001$ ) and tortuosity ( $P = .009$ ) depending on the type of arch. Comparisons within type of arch showed no change in angulation and tortuosity across proximal landing zones within type I arch ( $P = .349$  and  $P = .409$ ), and increases in angulation and tortuosity toward more distal proximal landing zones within type II ( $P = .003$  and  $P = .043$ ) and type III ( $P < .001$  in both).

**Conclusions:** The aortic arch classification is associated with a consistent geometric pattern of the aortic arch map, which identifies specific proximal landing zones with suboptimal angulation for stent graft deployment. Arches II and III also appear to have progressively less favorable anatomy for thoracic endovascular aortic repair compared with arch I. (*J Vasc Surg* 2017;■:1-7.)

Thoracic endovascular aortic repair (TEVAR) represents a well-established alternative to open repair in individuals with suitable anatomic features, particularly in patients considered at high surgical risk but with a reasonable life expectancy after the procedure.<sup>1</sup>

Feasibility assessment and subsequent preoperative planning of endovascular treatment are based on post hoc analysis of patient contrast-enhanced computed tomography (CT) images.<sup>2</sup> TEVAR requires healthy

proximal and distal landing zones of adequate diameter ( $<40$  mm) and length ( $\geq 20$  mm) and a viable iliofemoral or infrarenal aortic access route.<sup>2,3</sup> A steep aortic arch angulation, being considered highly predictive of endograft failure, represents a contraindication to TEVAR.<sup>3</sup> Notably, however, no consensus exists on how to measure and define critical arch angulations, with radius of curvature<sup>4</sup> being the method most commonly used in the instructions for use of commercially available endografts.

The actual planning of the endovascular procedure refers mainly to the identification of a proximal landing zone that provides adequate procedural safety and the greatest effectiveness and durability.<sup>3</sup> An insufficient proximal seal or an endograft migration, or both, lead invariably to an incomplete exclusion of the aortic pathology (ie, endoleak), with the inherent continued risk of aortic rupture, resulting in TEVAR clinical failure.<sup>5</sup> In this respect, the angulation of the proximal landing zone appears to be a crucial factor<sup>3</sup> because it increases the minimum length requirement of the landing zone for an effective deployment<sup>6</sup> and is associated with high displacement forces that increase the risk of endograft migration.<sup>7-9</sup> However, only heterogeneous definitions and methodology for measuring neck angulation have been reported thus far.<sup>10,11</sup>

Preoperative planning for endovascular repair of the aortic arch is described based on the aortic arch map reported by Ishimaru.<sup>12</sup> This classification defines the

From the Division of Vascular Surgery II,<sup>a</sup> Thoracic Aortic Research Center,<sup>b</sup> Division of Radiology,<sup>c</sup> and Department of Anesthesia and Intensive Care,<sup>d</sup> Istituto di Ricovero e Cura a Carattere Scientifico-Policlinico San Donato, San Donato Milanese; and the Department of Vascular Surgery, University Medical Center Utrecht, Utrecht.<sup>e</sup>

This work was supported in part by "Ricerca Corrente" and "5xmille" grants from Istituto di Ricovero e Cura a Carattere Scientifico-Policlinico San Donato, San Donato Milanese (MI), Italy.

Author conflict of interest: J.A.v.H. and F.L.M. served as consultants and received unrestricted grants from 3Mensio Medical Imaging B.V., Bilthoven, The Netherlands.

Correspondence: Massimiliano M. Marrocco-Trischitta, MD, PhD, Division of Vascular Surgery II, Thoracic Aortic Research Center, IRCCS-Policlinico San Donato, Via Morandi 30, San Donato Milanese (MI) 20097, Italy (e-mail: [massimiliano.marroccotrischitta@grupposandonato.it](mailto:massimiliano.marroccotrischitta@grupposandonato.it); [max\\_marrocco@yahoo.com](mailto:max_marrocco@yahoo.com)).

The editors and reviewers of this article have no relevant financial relationships to disclose per the JVS policy that requires reviewers to decline review of any manuscript for which they may have a conflict of interest.

0741-5214

Copyright © 2016 by the Society for Vascular Surgery. Published by Elsevier Inc. <http://dx.doi.org/10.1016/j.jvs.2016.10.113>

proximal landing zones (0 to 4) as related to the origin of the supra-aortic vessels and indicates the requirement of a prophylactic rerouting of the involved aortic branches, which can be performed with a surgical extra-anatomic bypass<sup>13</sup> or with endovascular procedures with the use of fenestrated or branched endografts<sup>14</sup> or with the chimney technique.<sup>15</sup> Ishimaru's aortic arch map, however, does not account for relevant critical anatomic features, including landing zone angulation and tortuosity,<sup>16,17</sup> arch elongation, which typically increases with age,<sup>18</sup> and branch vessel angulation.

Our aim was to assess whether the additional use of the aortic arch classification in type I, II, and III, originally developed for predicting difficult carotid stenting,<sup>19</sup> may complement the aortic arch map by providing valuable information on the geometry of the arch landing zones and suitability and planning for TEVAR.

## METHODS

This study reviewed anonymized thoracic CT angiography scans from patients undergoing diagnostic evaluation for various indications at our institution in 2015 and was approved by the local Ethic Committee. The need for patient informed consent was waived because of the retrospective nature of the analysis and the use of anonymized data.

Only thin-cut (1.0 mm or 1.5 mm) CTs of patients with a healthy aortic arch with visible origins of the supra-aortic branches were considered. Exclusion criteria were age <60 years, diameter of the thoracic aorta >40 mm, radius of arch curvature <20 mm, bovine arch, previous aortic surgery, and presence of radiologic signs of aortic dissection, intramural hematoma, or penetrating aortic ulcer. Aneurysmatic aortas were excluded because the original description of the aortic arch classification<sup>19</sup> was based on healthy aortas. Aortas with radius of curvature <20 mm were excluded because the latter defines a steep aortic arch angulation that could alter the measurements of the proximal landing zone angulation and represents a contraindication to TEVAR, according to instructions for use of stent graft manufacturers. Bovine arches were excluded because this anatomic configuration does not allow a reproducible definition of Ishimaru's aortic arch map.

Suitable cases were stratified according to aortic arch classification.<sup>19</sup> In detail, the diameter of the left common carotid artery was measured at its origin in axial view. Multiplanar reconstruction images were then used to create a parasagittal view for each scan to visualize the origin of the brachiocephalic trunk and the top of the aortic arch in one frame. Finally, the distance between the origin of the brachiocephalic trunk and the top of the arch was used to classify each case as a type I, type II, or type III arch (Fig 1). Two observers (H.W.d.B. and F.S.) independently assessed CT scans for exclusion and inclusion criteria. Overall, 20 cases of each type of arch were selected.

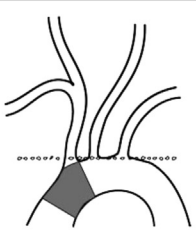
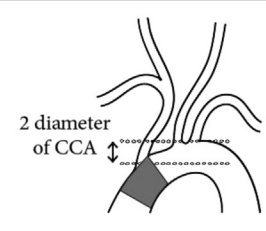
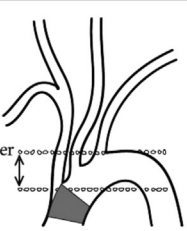
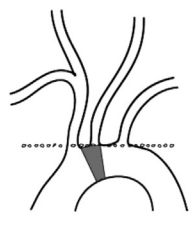
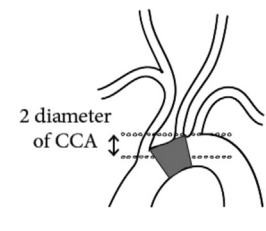
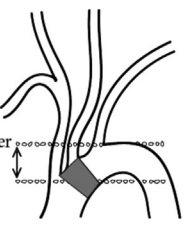
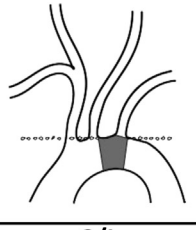
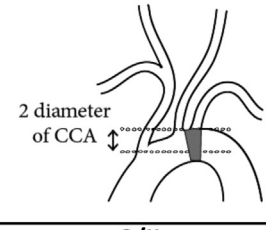
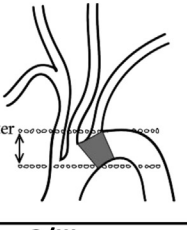
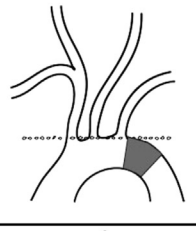
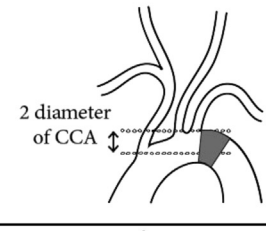
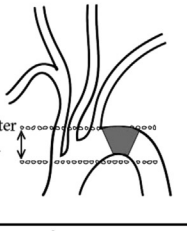
## ARTICLE HIGHLIGHTS

- **Significance:** The authors investigate whether a combination of two standard aortic arch classifications is clinically useful for preoperative planning of thoracic endovascular aortic repair.
- **Type of Research:** Retrospective single center cohort study
- **Take Home Message:** Type II and type III aortic arches are associated with greater angulation, especially in aortic landing zones 2 and 3.
- **Recommendation:** The authors suggest to combine Ishimaru's aortic arch map classification of landing zones 0-3 with the aortic arch classification of types I to III to better plan thoracic endovascular aortic repair.
- **Strength of Recommendation:** 2. Weak
- **Level of Evidence:** C. Low or very low

Further processing, based on three-dimensional multiplanar reconstruction, was performed with 3Mensio Vascular 8.0 software (3Mensio Medical Imaging B.V., Bilthoven, The Netherlands), which provides specific functions for automatic measurements. Four markers (A-D) were placed in axial view at the level of the top of the pulmonary artery bifurcation. Points A and B are a midluminal point of the ascending and descending aorta at the height of the bifurcation of the pulmonary trunk. Points C and D are two points within the same plane where the distance between the ascending aorta and descending aorta is the smallest (Fig 2). Different variables were then measured as follows:

The radius of arch curvature was defined as half of the shortest distance between C and D (Fig 2, A). The aortic arch tortuosity index was defined as shortest distance between A and B divided by the center lumen line distance between A and B (Fig 2, B). Center lumen line lengths of each landing zone were measured in view perpendicular to the center lumen line (Fig 2, C). Zone 0 was measured starting from level of the top of the pulmonary artery bifurcation because this marks the beginning of the arched part of the ascending aorta. Zone 3 by definition has a length of 20 mm. The ratio of the outer curvature length to the center lumen line length of the arch (ie, between point A and B) was measured with the outer curvature function (Fig 2, D).

The angle between the flow axis of each proximal landing zone and the hypothetical body of the lesion to treat, analogous to the  $\beta$  angle as defined in the Society for Vascular Surgery reporting standards for endovascular abdominal aorta repair (EVAR),<sup>20</sup> was determined. For this purpose, the center lumen line tangent angle function was used, which calculates the angle between tangent lines drawn for any two points along the center lumen line (Fig 3, A). The  $\beta$  angles of each proximal

	Type I	Type II	Type III
Zone 0			
MALAN	0/I	0/II	0/III
Zone 1			
MALAN	1/I	1/II	1/III
Zone 2			
MALAN	2/I	2/II	2/III
Zone 3			
MALAN	3/I	3/II	3/III

**Fig 1.** The newly proposed modified arch landing areas nomenclature (MALAN), which comprises the proximal landing zones according to the Ishimaru aortic arch map<sup>12</sup> and types of arch according to the aortic arch classification.<sup>19</sup> CCA, Common carotid artery.

landing zone were calculated by selecting the most proximal point of the zone and a point at 40 mm distance along the center lumen line. The more proximal 20 mm of such a distance accounted for the proximal neck and the more distal 20 mm for the hypothetical body of the lesion to treat. For zone 0, the proximal point was selected at the level of the top of the pulmonary trunk. The  $\beta$  angles were independently measured by two blinded investigators (H.W.d.B. and T.M.v.B.) and classified into cases of mild ( $<40^\circ$ ), moderate ( $40^\circ$ - $60^\circ$ ), or severe ( $>60^\circ$ ) angulation.<sup>2,21</sup>

The tortuosity angle of each landing zone was measured using the tortuosity angle function that is incorporated in the 3Mensio software. According to the manufacturer, this is measured between two line elements that are defined by three control points that are all on the centerline: The first point is the start of the first line element, the second point is the end of the first line element and the start of the second line element, and the third point is the end of the second line element. The distance between the points can be changed along the centerline, and was set at 20 mm for the purpose of

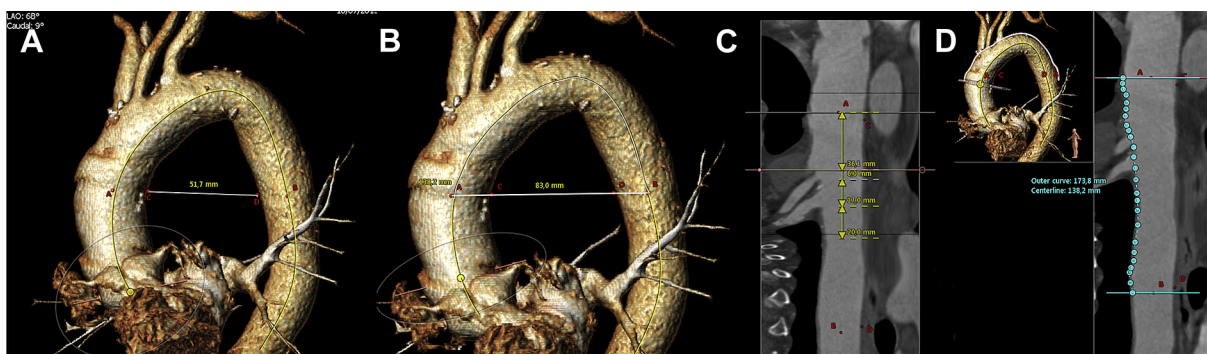


**Fig 2.** **A**, Radius of arch curvature. **B**, Aortic arch tortuosity index. **C**, Center lumen line lengths. **D**, Ratio of outer curvature length to center lumen line length (see [Methods](#) for details).

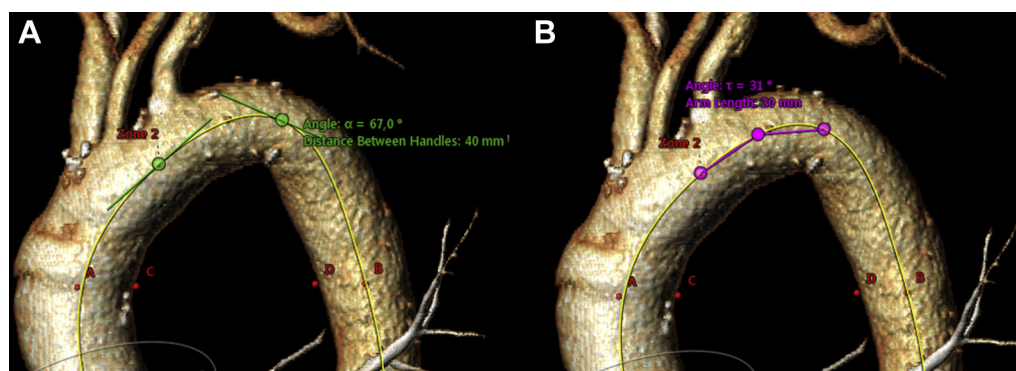


**Fig 3.** **A**,  $\beta$  angles<sup>20</sup> (green lines) of the proximal landing zone, as defined as  $\alpha$  by 3Mensio Vascular 8.0 software (3Mensio Medical Imaging B.V., Bilthoven, The Netherlands). **B**, Tortuosity angle of proximal landing zone (red lines; see [Methods](#) for details).

our study because this was considered the minimum landing zone length ([Fig 3, B](#)).

Measurements were repeated for 10 scans (16.7%) randomly selected from the study group to assess intra-observer and interobserver repeatability using Bland-Altman plots.

Data are described according to a modified arch landing areas nomenclature (MALAN) that comprises Ishimaru's proximal landing zones and type of arch (eg O/I; [Fig 1](#)).

**Statistical analysis.** Data were analyzed using SPSS Statistics 22 software (IBM Corp, Armonk, NY). Normality was tested with the Shapiro-Wilk test, after which a comparison between the types of arch was made with one-way analysis of variance for normally distributed data and with the Kruskal-Wallis test for non-normally distributed data. The Jonckheere-Terpstra test was used to compare the angulation and tortuosity across landing zone within each type of arch. Continuous data are shown as the mean  $\pm$  standard deviation. Statistical significance was assumed at  $P < .05$ .

## RESULTS

The 60 selected patients (70% male) were  $71 \pm 8$  years old. The three groups defined by the type of arch were

comparable in age (type I:  $78.8 \pm 8.5$  years; type II:  $75.2 \pm 8.5$  years; type III:  $75.4 \pm 9.5$  years;  $P = .291$ ) and radius of curvature ([Table 1](#)). No differences were found between the center lumen line and outer curvature measurements ([Table 1](#)), which exclude potential bias for measurements of proximal landing zones length. Landing zones length values were comparable between types of arch ([Table 1](#)), which in turn exclude bias for measurements of  $\beta$  angles.

Angulation and tortuosity of the arch landing areas, defined according to the MALAN classification ([Fig 1](#)), are reported in [Tables II](#) and [III](#).

The absolute values<sup>2,21</sup> for angulation were moderate in O/I, 1/I, 2/I, and 3/I, and in O/II, 1/II, 2/II, and 3/II. Angulation was moderate in O/III and in 1/III and was severe in 2/III and in 3/III.

Comparisons between types of arch showed a significant increase in landing zones angulation depending on the type of arch ( $P < .001$ ). Of note, 2/II was significantly more angulated than 2/I ( $+12.0^\circ$ ;  $P = .012$ ), 2/III was more angulated than 2/I ( $+17.2^\circ$ ;  $P < .001$ ), and 3/III was more angulated than 3/II ( $+13.3^\circ$ ;  $P = .003$ ) and 3/I ( $+18.3^\circ$ ;  $P < .001$ ).

Comparisons within the types of arch showed no change in angulation across landing zones within the type I arch ( $P = .349$ ), whereas significant increases in

**Table I.** Comparison of general indexes of arch angulation

Variables <sup>a</sup>	Type I	Type II	Type III	P
Radius of curvature	30.6 ± 6.5	29.0 ± 6.4	27.3 ± 4.6	.270
Aortic arch center lumen line length	141.3 ± 22.6	128.2 ± 15.6	130.8 ± 33.9	.153
Aortic arch outer curvature length	166.0 ± 46.2	165.4 ± 19.2	173.5 ± 24.5	.617
Ratio of outer curvature to center lumen line	1.26 ± 0.04	1.29 ± 0.05	1.28 ± 0.04	.155
Aortic arch tortuosity index	1.48 ± 0.12	1.45 ± 0.18	1.57 ± 0.21	.082
Center lumen line length				
Zone 0	35.5 ± 8.7	32.5 ± 5.9	35.6 ± 7.9	.356
Zone 1	9.3 ± 2.8	9.7 ± 2.7	8.3 ± 3.0	.281
Zone 2	16.4 ± 4.6	16.7 ± 4.9	16.7 ± 2.9	.967
Zone 3	20.0	20.0	20.0	

<sup>a</sup>Data are presented as mean ± standard deviation. Values are lengths in mm.

**Table II.** Angulation ( $\beta$  angle) of modified arch landing areas nomenclature (MALAN) areas with comparisons across landing zone and type of arch

Zone <sup>a</sup>	Type I	Type II	Type III	P
0	0/I: 48.6 ± 11.3	0/II: 44.3 ± 10.5	0/III: 39.7 ± 11.2	.046
1	1/I: 41.9 ± 14.5	1/II: 50.8 ± 14.4	1/III: 52.3 ± 12.0	.040
2	2/I: 44.5 ± 14.7	2/II: 56.4 ± 16.8	2/III: 61.7 ± 11.6	.001
3	3/I: 52.9 ± 11.8	3/II: 52.3 ± 14.9	3/III: 71.1 ± 14.1	<.001
P	.349	.003	<.001	

<sup>a</sup>Data are presented as mean ± standard deviation. Values are in degrees.

**Table III.** Tortuosity (tortuosity angle) of modified arch landing areas nomenclature (MALAN) areas with comparisons across landing zone and type of arch

Zone <sup>a</sup>	Type I	Type II	Type III	P
0	0/I: 23.9 ± 8.6	0/II: 25.9 ± 6.9	0/III: 20.8 ± 5.9	.088
1	1/I: 22.0 ± 7.2	1/II: 23.1 ± 8.8	1/III: 23.1 ± 8.8	.732
2	2/I: 24.2 ± 10.3	2/II: 29.2 ± 12.8	2/III: 29.2 ± 6.4	.213
3	3/I: 25.9 ± 8.1	3/II: 30.7 ± 8.5	3/III: 39.5 ± 8.2	<.001
P	.409	.043	<.001	

<sup>a</sup>Data are presented as mean ± standard deviation. Values are in degrees.

angulation were observed toward more distal landing zones within the type II ( $P = .003$ ) and type III ( $P < .001$ ) arches. Between adjacent landing areas, 3/III was more angulated than 2/III (+9.5°;  $P = .017$ ), 2/III was more angulated than 1/III (+9.4°;  $P = .018$ ), and 1/III was more angulated than 0/III (+12.6°;  $P = .002$ ).

The tortuosity index did not differ between types of arch (Table I). In contrast, comparisons in tortuosity angles between types of arch showed a significant trend of increased landing zone tortuosity across type of arch ( $P = .009$ ). Of note, 3/III was more tortuous than 3/II (+8.8°;  $P = .001$ ) and 3/I (+13.6°;  $P < .001$ ).

Comparisons within types of arch showed no change in tortuosity angles across landing zones within the type I arch ( $P = .409$ ), whereas there were significant increases in tortuosity toward more distal landing zones within

the type II ( $P = .043$ ) and type III ( $P < .001$ ) arches. Between adjacent landing areas, 3/III was more tortuous than 2/III (+10.3°;  $P < .001$ ), and 2/III was more tortuous than 1/III (+5.2°;  $P = .025$ ).

Mean intraobserver and interobserver differences for the  $\beta$  angle measurements were 0.6° ± 9.3° ( $P = .677$ ) and 0.6° ± 8.1° ( $P = .643$ ), respectively.

## DISCUSSION

Our analysis showed that the aortic arch classification is associated with a consistent geometric pattern of Ishimaru's zones that identifies specific proximal landing areas with suboptimal angulation and tortuosity for stent graft deployment. Also, type II and type III arches appear to have progressively less favorable anatomy for TEVAR compared with type I.

The geometric variability of the aortic arch and of its branches represents a critical issue for preprocedural planning of TEVAR.<sup>2,3,21</sup> In fact, a planning based exclusively on the Ishimaru aortic map<sup>12</sup> disregards the influence of angulation and tortuosity of the landing zones and would be valid only under the assumption that these anatomic features are constant through the arch, which our results show applies only to type I arch.

The concept of establishing an absolute optimal value for proximal landing zone length is based on this assumption. However, this value varies in the literature between 15 and 30 mm,<sup>22</sup> and such a discrepancy confirms that other factors interfere with optimal neck length<sup>22</sup> and, particularly, a localized angulation.<sup>6</sup> Previous studies showed that the landing zones with greater angulation must be greater in length to provide an adequate sealing and fixation.<sup>6</sup> In the aortic arch, this implies that when a longer neck is required, a more proximal aortic landing zone should be chosen. In this respect, 2/III and 3/III areas, as defined according to the newly proposed MALAN classification, appear hostile from a geometric standpoint as proximal landing zones.

Another relevant issue is the effect of aortic angulation on the risk of graft migration<sup>21</sup> because it represents an important determinant of the magnitude of the displacement forces acting on the stent graft after its deployment.<sup>9</sup> In fact, rather than taking into account only the value of the localized angulation of the actual landing zone, the whole arch should be considered because neck angulations proximal to the landing zone may also influence migration forces to some degree.<sup>9</sup> Therefore, 2/II and 3/II areas, despite being associated with moderate angulations, could also actually be suboptimal landing zones<sup>9</sup> because type II arch angulation increases progressively toward the distal part of the arch. Further studies currently in progress, based on computational fluid dynamics, will show whether the geometric patterns described by the MALAN classification are associated with different magnitude and direction of migration forces.

Tortuosity of the aorta is another relevant anatomic feature that is associated with higher rates of type II endoleaks, probably due to a reduced contact surface between the endograft and the native aorta.<sup>16</sup> Also, an increased risk of stroke has been reported, likely related to the need of a greater perioperative manipulation and the risk of dislodgment of the arch atheroma caused by the increased mechanical stress induced by the endograft on the outer aortic curvature.<sup>16</sup> Even more importantly, however, tortuosity in the proximal and distal fixation zones was reported to be associated with type I endoleak.<sup>17</sup> In this respect, our data show that 2/III and 3/III, as well as 2/II and 3/II areas, appear again suboptimal as proximal landing zones.

Finally, the newly proposed nomenclature may be useful also for assessment of the feasibility of fenestrated

endografting of the arch. The take-off angles of the supra-aortic branches predict a difficult cannulation, consistently with the original description of the classification,<sup>19</sup> and may expose the bridging stents to increased mechanical stress and affect seal at the fenestrations.

In the present study, we sought to elaborate an original nomenclature for aortic arch areas by using well-established and widely shared definitions. Consistently, because for TEVAR there is no consensus on how to measure the angulation of the proximal landing zones or on the threshold angulation values for a safe and effective endograft deployment, we used methods and angle grades previously validated for EVAR,<sup>2,20</sup> even though we are aware of the hemodynamic differences between the thoracic and the abdominal aorta.<sup>23</sup>

As a result, the proposed MALAN classification has a readily intuitive interpretation based on viewing the aorta during planning in the parasagittal plane, which notably is also the plane required intraoperatively for stent graft deployment. Also, geometric calculations are not required, which can be complex and time consuming and may even introduce a further possible source of bias unless a standardized protocol is used.<sup>24</sup>

## CONCLUSIONS

We recognize that our data need to be validated in pathologic aortas, namely in patients who undergo TEVAR, in whom also the clinical relevance of our observations have to be proven by a postoperative outcome analysis. Another limitation of evaluating healthy aortas is the use of a hypothetical body of the lesion to treat for the calculation of  $\beta$  angles. Nevertheless, we believe that the newly introduced nomenclature provides at glance useful insights for assessing TEVAR feasibility and planning and represents a promising tool to improve the preoperative decision making process.

## AUTHOR CONTRIBUTIONS

Conception and design: MM-T, HdB, FS, TvB, MR, ST  
 Analysis and interpretation: MM-T, HdB, FS, TvB, MR, JvH, FM, ST  
 Data collection: MM-T, HdB, FS, TvB, MR  
 Writing the article: MM-T, HdB, MR, ST  
 Critical revision of the article: MM-T, HdB, FS, TvB, MR, JvH, FM, ST  
 Final approval of the article: MM-T, HdB, FS, TvB, MR, JvH, FM, ST  
 Statistical analysis: HdB, MR  
 Obtained funding: MM-T, ST  
 Overall responsibility: MM-T

## REFERENCES

1. Marrocco-Trischitta MM, Melissano G, Kahlberg A, Calori G, Setacci F, Chiesa R. Chronic kidney disease classification stratifies mortality risk after elective stent graft repair of the thoracic aorta. *J Vasc Surg* 2009;49:296-301.

2. Erbel R, Aboyans V, Boileau C, Bossone E, Di Bartolomeo R, Eggebrecht H, et al. 2014 ESC Guidelines on the diagnosis and treatment of aortic diseases: document covering acute and chronic aortic diseases of the thoracic and abdominal aorta of the adult. The Task Force for the Diagnosis and Treatment of Aortic Diseases of the European Society of Cardiology (ESC). *Eur Heart J* 2014;35:2873-926.
3. Grabenwoger M, Alfonso F, Bachet J, Bonser R, Czerny M, Eggebrecht H, et al. Thoracic endovascular aortic repair (TEVAR) for the treatment of aortic diseases: a position statement from the European Association for Cardio-Thoracic Surgery (EACTS) and the European Society of Cardiology (ESC), in collaboration with the European Association of Percutaneous Cardiovascular Interventions (EAPCI). *Eur Heart J* 2012;33:1558-63.
4. Muhs BE, Balm R, White GH, Verhagen HJ. Anatomic factors associated with acute endograft collapse after Gore TAG treatment of thoracic aortic dissection or traumatic rupture. *J Vasc Surg* 2007;45:655-61.
5. Fillinger MF, Greenberg RK, McKinsey JF, Chaikof EL; Society for Vascular Surgery Ad Hoc Committee on TEVAR Reporting Standards. Reporting standards for thoracic endovascular aortic repair (TEVAR). *J Vasc Surg* 2010;52:1022-33.
6. Altnji HE, Bou-Saïd B, Walter-Le Berre H. Morphological and stent design risk factors to prevent migration phenomena for a thoracic aneurysm: a numerical analysis. *Med Eng Phys* 2015;37:23-33.
7. Geisbusch P, Kotelis D, Hyhlik-Durr A, Hakimi M, Attigah N, Bockler D. Endografting in the aortic arch e does the proximal landing zone influence outcome? *Eur J Vasc Endovasc Surg* 2010;39:693-9.
8. Figueroa CA, Taylor CA, Yeh V, Chiou AJ, Zarins CK. Effect of curvature on displacement forces acting on aortic endografts: a 3-dimensional computational analysis. *J Endovasc Ther* 2009;16:284-94.
9. Molony DS, Kavanagh EG, Madhavan P, Walsh MT, McGloughlin TM. A computational study of the magnitude and direction of migration forces in patient-specific abdominal aortic aneurysm stent-grafts. *Eur J Vasc Endovasc Surg* 2010;40:332-9.
10. Boufi M, Guivier-Curien C, Deplano V, Boiron O, Loundou AD, Dona B, et al. Risk factor analysis of bird beak occurrence after thoracic endovascular aortic repair. *Eur J Vasc Endovasc Surg* 2015;50:37-43.
11. Sweet MP. Anatomic features of the distal aortic arch that influence endovascular aneurysm repair. *J Vasc Surg* 2016;64:891-5.
12. Ishimaru S. Endografting of the aortic arch. *J Endovasc Ther* 2004;11(Suppl 2):162-71.
13. Antoniou GA, El Sakka K, Hamady M, Wolfe JH. Hybrid treatment of complex aortic arch disease with supra-aortic debranching and endovascular stent graft repair. *Eur J Vasc Endovasc Surg* 2010;39:683-90.
14. Greenberg R, Eagleton M, Mastracci T. Branched endografts for thoracoabdominal aneurysms. *J Thorac Cardiovasc Surg* 2010;140(Suppl):S171-8.
15. Kolvenbach RR, Rabin A, Karmeli R, Alpaslan A, Schwierz E. Developments in parallel grafts for aortic arch lesions. *J Cardiovasc Surg* 2016;57:448-56.
16. Chen CK, Liang IP, Chang HT, Chen WY, Chen IM, Wu MH, et al. Impact on outcomes by measuring tortuosity with reporting standards for thoracic endovascular aortic repair. *J Vasc Surg* 2014;60:937-44.
17. Ueda T, Takaoka H, Raman B, Rosenberg J, Rubin GD. Impact of quantitatively determined native thoracic aortic tortuosity on endoleak development after thoracic endovascular aortic repair. *AJR Am J Roentgenol* 2011;197:W1140-6.
18. Redheuil A, Yu WC, Mousseaux E, Harouni AA, Kachenoura N, Wu CO, et al. Age-related changes in aortic arch geometry: relationship with proximal aortic function and left ventricular mass and remodeling. *J Am Coll Cardiol* 2011;58:62-70.
19. Madhwal S, Rajagopal V, Bhatt DL, Bajzer CT, Whitlow P, Kapadia SR. Predictors of difficult carotid stenting as determined by aortic arch angiography. *J Invasive Cardiol* 2008;20:200-4.
20. Chaikof EL, Fillinger MF, Matsumura JS, Rutherford RB, White GH, Blankensteijn JD, et al. Identifying and grading factors that modify the outcome of endovascular aortic aneurysm repair. *J Vasc Surg* 2002;35:1061-6.
21. Sternbergh WC 3rd, Carter G, York JW, Yoselevitz M, Money SR. Aortic neck angulation predicts adverse outcome with endovascular abdominal aortic aneurysm repair. *J Vasc Surg* 2002;35:482-6.
22. Boufi M, Aouini F, Guivier-Curien C, Dona B, Loundou AD, Deplano V, et al. Examination of factors in type I endoleak development after thoracic endovascular repair. *J Vasc Surg* 2015;61:317-23.
23. Xiao N, Humphrey JD, Figueroa CA. Multi-scale computational model of three-dimensional hemodynamics within a deformable full-body arterial network. *J Comput Physiol* 2013;244:22-40.
24. van Keulen JW, Moll FL, Tolenaar JL, Verhagen HJ, van Herwaarden JA. Validation of a new standardized method to measure proximal aneurysm neck angulation. *J Vasc Surg* 2010;51:821-8.

Submitted Aug 26, 2016; accepted Oct 30, 2016.